submitted to Journal of Climate

A Mechanism for the High Rate of Sea-Ice Thinning in the Arctic Ocean

C. M. Bitz [1] and G. H. Roe [2]

Abstract. Submarine measurements of sea ice draft show that the ice has thinned in some parts of the Arctic Ocean at a remarkably high rate over the past few decades. The spatial pattern indicates the thinning was a strong function of ice thickness, with the greatest thinning having occurred where the ice was thickest initially. A similar relationship between sea ice thinning and the initial thickness is reproduced individually by three global climate models in response to increased levels of carbon dioxide in the models' atmosphere. All three models have weak trends in their surface winds and one model lacks ice dynamics altogether, implying that trends in the atmosphere or ice circulation are not necessary to produce a relatively high rate of thinning over the central Arctic or a thickness change that increases with the initial thickness. We develop a general theory to describe the thinning of sea ice subject to climate perturbations. We find that the leading component of the thickness-dependence of the thinning is due to the basic thermodynamics of sea ice. When perturbed, sea ice returns to its equilibrium thickness by adjusting its growth rate. The growth-thickness relationship is stabilizing and hence can be reckoned a negative feedback. The feedback is stronger for thinner ice, which is known to adjust more quickly to perturbations than thicker ice. In addition, thinner ice need not thin much to increase its growth rate a great deal, thereby establishing a new equilibrium with relatively little change in thickness. In contrast, thicker ice must thin much more. An analysis of a series of models, with physics ranging from very simple to highly complex, indicates that this growth-thickness feedback is the key to explaining the models' relatively high rate of thinning in the central Arctic compared to thinner ice in the subpolar seas.

1. Introduction

Recent submarine-based measurements indicate that the thickness of sea ice in some parts of the central Arctic has decreased at a remarkably high rate over the past few decades [Rothrock et al., 1999; Wadhams and Davis, 2000]. Based on their analysis of sonar reflections from the ice draft, Rothrock et al. [1999] concluded that the ice thinned by about 1.3 m in the 1990's relative to the period 1958–76 by comparing all overlapping submarine tracks between the two periods. A further intriguing aspect of these data is that the measured thinning is a strong function of the draft. Figure 1 shows the reduction in ice draft for each location where a submarine track from the 1990s crossed a track from the period 1958–76, as a function of the mean ice draft in the same location in 1958–76, based on data from Rothrock et al. [1999]. The reduction in draft increases roughly linearly with the initial draft.

This relationship is in striking contrast to the situation on seasonal timescales, where the largest change in the mass balance of sea ice occurs for thin ice. Thin ice tends to experience high melt rates in summer due to ice-albedo feedback, and thin ice may also grow rapidly in winter when it can conduct a great deal of heat from the ocean to the atmosphere. Clearly the thickness-dependence of the thinning on decadal timescales shown in Fig. 1 is not due to ice-albedo feedback. Nor does Fig. 1 show that the reduction in thickness is merely limited by the ice available to melt.

Several recent studies argue that changes in the atmospheric circulation are chiefly responsible for the thickness change measured by the submarines [Tucker et al., 2001; Holloway and Sou, 2002; Rothrock et al., 2003]. Holloway and Sou [2002] hypothesized that the thickness change averaged over the limited area measured by submarines is larger than the basin average owing to a redistribution of ice by surface winds. Their model results show ice diverged out of the region sampled by the submarines and converged near the Canadian Archipalego, outside of the submarine data boundary. Modelers also find that the Arctic sea ice volume is more responsive to recent wind stress anomalies than to recent atmospheric heat flux anomlies [Zhang et al., 2000; Holloway and Sou, 2002; Köberle and Gerdes, 2003]. If recent basin-scale (∼1000 km) thickness change is primarily due to winds, it is natural to ask if the sub-basin scale distribution of thickness change (i.e., on the scale of the separation of the 29 submarine crossings, or ∼100 km and smaller) is also due to winds.

[1]Polar Science Center, University of Washington
[2]Earth and Space Sciences, University of Washington

And if so, is the apparent thickness-dependence in Fig. 1 due to changes in the winds as well? Unfortunately sea ice models are only moderately successful at reproducing the spatial pattern of the thickness in a given year [Rothrock et al., 2003, see their Fig. 7] or the spatial pattern of thickness change measured by submarines [Holloway and Sou, 2002], and so this question cannot easily be answered.

In this study we consider an alternative explanation, we show that the inherent properties of sea ice give rise to a strongly thickness-dependent sensitivity to perturbations, whether due to anomalous wind or ocean stresses or surface heat fluxes. We show that coupled climate models exhibit roughly the same relationship between ice thinning and the initial thickness as shown in Fig. 1 when subject to increasing levels of carbon dioxide in the models' atmosphere. These models have a wide variety of physical formulations for sea ice (some are motionless while others have ice dynamics that account for the material properties of ice), but they all represent the same basic thermodynamics of sea ice. With this motivation, we present a mechanism based only on the thermodynamics of sea ice to explain how sea ice can thin most where the ice was initially thickest. We also develop a general theory, which accounts for ice dynamics as well as thermodynamics, to describe the equilibrium thickness sensitivity of sea ice to changes in forcing.

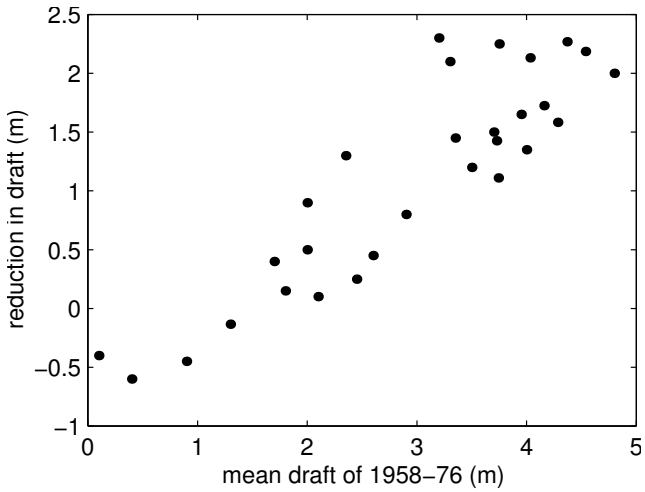

Figure 1. Scatter plot of the reduction in ice draft between two periods: 1993–1997 and 1958–76 as a function of the mean draft from the earlier period. Data are from the submarine measurements and analysis presented in Rothrock et al. [1999] and were kindly provided by Y. Yu. As explained in Rothrock et al. [1999], the cruises took place between late July and late October, so the data have been seasonally adjusted to September 15 using an estimate of the climatological mean annual cycle of sea ice thickness from a model. The thickness reduction is significantly correlated ($R = 0.89$) to the initial thickness, assuming the 29 points are independent, with probability greater than 99%.

2. Ice-thickness change in CMIP models

We first present the ice-thickness change simulated by three coupled climate models each with very different sea ice physics from the others. Each model was forced identically with increasing CO_2 at the rate of 1% per year as part of the Coupled Model Intercomparison Project (CMIP) [Meehl et al., 2000]. We found similar results in each of the 14 CMIP models we examined, but selected just three to demonstrate our point. The first model is the Community Climate System Model version 2 (CCSM2), which has the most sophisticated sea ice physics: Ice dynamics are computed assuming a viscous plastic rheology, a sub-gridscale ice-thickness distribution is parameterized with explicit deformation and redistribution, and heat storage in brine pockets is computed explicitly [Briegleb et al., 2002]. The second model is the Hadley Centre Climate Model version 3 (HadCM3). The sea ice in HadCM3 [Gordon et al., 2000] has an intermediate level of complexity among the three models, with ice motion derived solely from ocean currents and thermodynamics based on the Semtner three-layer method [Semtner, 1976]. The Max-Planck-Institut fuer Meteorlogie Model version 3 (ECHAM3-LSG) has the simplist sea ice, which is motionless and neglects heat storage in ice altogether [Cubasch et al., 1997].

A more complete presentation of the simulations of Arctic climate change in the CMIP models is given by Holland and Bitz [2003] and Flato [2004]. Here we analyize the models specifically to see if they reproduce the relationship between thinning and initial thickness that is apparent from submarine measurements.

Flato [2004] noted that the spatial pattern of thinning in global climate models tends to have a maximum somewhere in the central Arctic. This is illustrated for each of the three models in Fig. 2 (left column), which shows that the zonal mean thickness in the control (present day CO_2 level) and perturbed (at twice the present day CO_2 level) simulations. In all cases the greatest thinning occurs where the ice is thickest, which in the zonal mean, lies in the central Arctic.

We also show scatter plots (right column in Fig. 2) of the spatial distribution of the reduction in thickness as a function of the control thickness for the three models. The points in Fig. 2 are taken for all gridcells north of 70°N to roughly represent the central Arctic, but the scatter plots for all gridcells in the northern hemisphere (not shown) look similar. The scatter plots resemble Fig. 1 in that the thickness reduction in the models also increases with initial thickness (i.e., from the control case). The global average of the radiative forcing

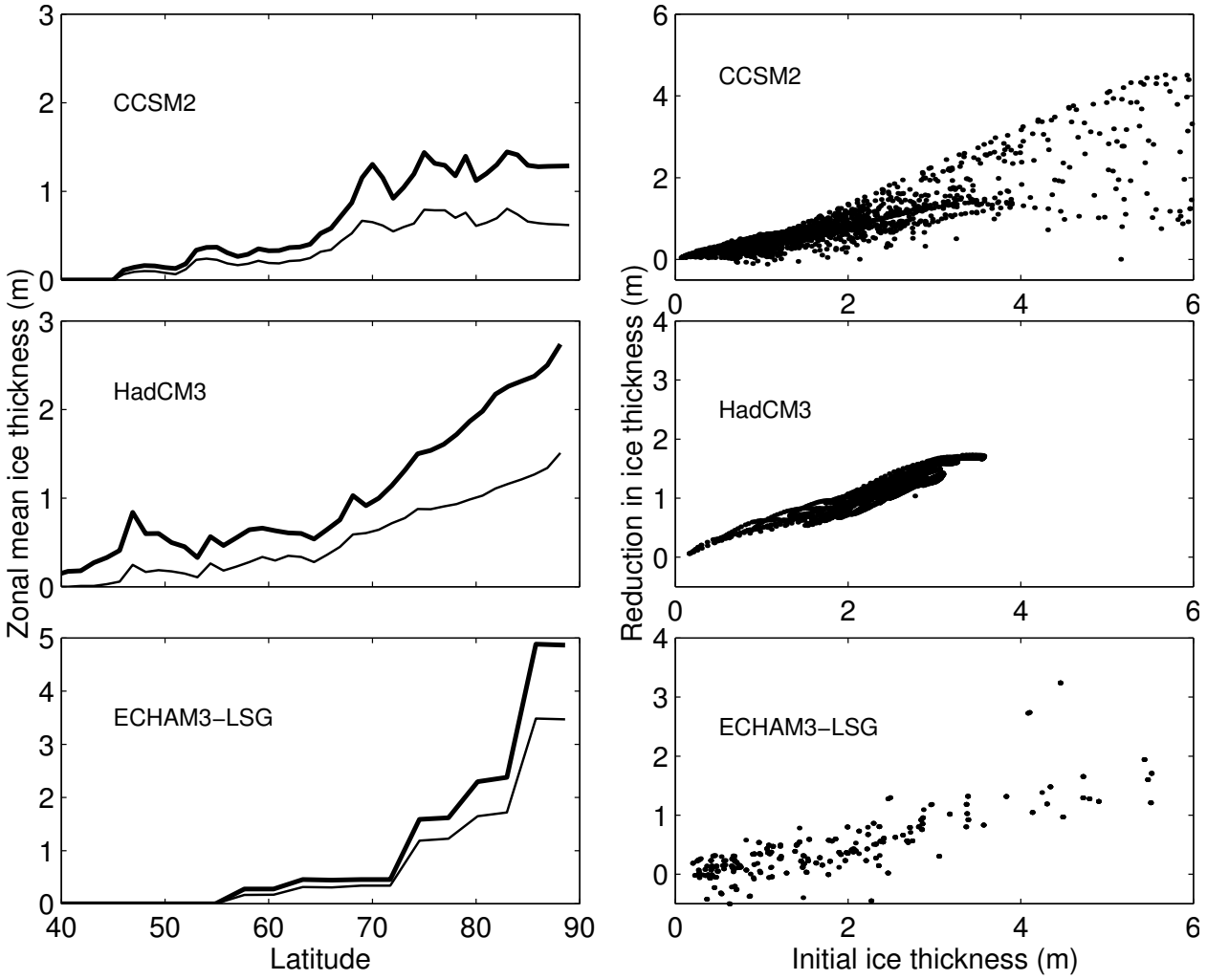

Figure 2. Zonal mean thickness (left column) in the control (thick lines) and perturbed (thin lines) simulations and scatter plots (right column) of the reduction in thickness as a function of the control (or initial) thickness taken from each gridcell in the northern hemisphere where the ice concentration exceeds 15% (CCSM2 and HADCM3) or the thickness exceeds 15cm (ECHAM3) in the initial simulation. The control climate thickness is an 80-yr mean from an integration with CO_2 held fixed at present day levels, and the perturbed climate thickness is a 20-yr mean about the time of doubling CO_2 over the present day level.

increase from doubling CO_2, which was prescribed in the perturbed case of the CMIP models, is about three and a half times greater than estimates of the direct radiative forcing increase that has occurred in the interval between the submarine measurements (based on the work of Hansen et al., 2002), and yet the thickness change for a given thickness is about the same in the models and as measured by the submarines. This suggests that the models appear to miss some aspect of the recent change. One thing we know for certain is that the trends in the surface winds are much weaker in most CMIP models compared to recent observed trends [Gillett et al., 2002]. In spite of the likely differences in the source of the thickness perturbation (i.e., suface radiative fluxes in the CMIP models and mostly wind stress in nature) the relationship between the resulting thickness change and the thickness is nearly the same.

The thickness change and control thickness shown in Fig. 2 are taken from annual mean output from the models, while the submarine data in Fig. 1 are from September. Because the same basic relationship emerges from each, we infer that with regard to the physics of the thickness change, there is probably nothing special about September in the observations. Furthermore the relationship between the change and initial state extends to firstyear ice (ice that does not survive summer melt) in the models.

Table 1. Variable definitions for the analytic model

	Variables	
h	Annual mean ice thickness	variable
T	Winter mean ice surface temperature in Celsius	variable
A	σT_f^4 with T_f=273K	320 Wm^{-2}
B	$4\sigma T_f^3$	4.6 Wm^{-2}
D	Atmospheric heat transport	100 Wm^{-2}
F_{SW}	Summer mean shortwave insolation 68 or 80°N	175 or 200 Wm^{-2}
F_W	Ocean heat flux	2 Wm^{-2}
L	Latent heat of fusion	3x10^8 J m^{-3}
k	Thermal conductivity	2 W m^{-1} K^{-1}
$n_{w,s}$	Optical depth for winter or summer	2.5 or 3.25
α	Sea ice albedo	0.65
σ	Stefan-Boltzmann constant	5.6e-8 W m^{-2} K^{-4}
τ	One-half year	182.5 days

3. Sea ice growth as a feedback on thickness

The common behavior among the CMIP models, some of which have motionless sea ice, suggests that the basic thermodynamics of sea ice alone must play a dominant role. The mechanism we propose follows from a simple line of reasoning. It has long been known that when perturbed, sea ice returns to its equilibrium (or quasi-equilibrium) thickness by adjusting its growth rate (see e.g., Untersteiner, 1961 and 1964). The rate at which ice can respond to a perturbation in forcing, (i.e., the response time) depends on the growth adjustment process. Using a simplified analytical model, Thorndike [1992] found that the response time of sea ice is about 3 yrs for 1 m thick ice, and he noted that the response time increases with ice thickness. Here we take these ideas one step further to consider the thickness-dependence of the equilibrium thickness change in response to a perturbation in the climate forcing. These results are directly analogous to Hansen et al. [1985], who showed that systems with long response times also experience a large equilibrium temperature change in response to radiative forcing. If sea ice behaves in a similar way, both the equilibrium thickness change and the response time should increase with thickness.

We begin by considering the mass budget of a sea ice floe. The ice attains an equilibrium thickness h_{eq} when the annually accumulated growth G and melt M balance under climatological mean conditions, provided the floe remains within a similar climatic region long enough. Theoretical efforts to compute the equilibrium thickness can lead to rather complex equations (see e.g., Kolesnikov, 1958). Instead we use the simplified analytic model of Thorndike [1992], which includes only the barest elements of the climate system in order to allow tractable analytic expressions for G and M. This model neglects the motion of sea ice altogether, thereby assuming the ice can always establish an equilibrium thickness. In following sections we consider the errors due to some of the assumptions made for this analytical model by analyzing the behavior of sea ice in more complex numerical models.

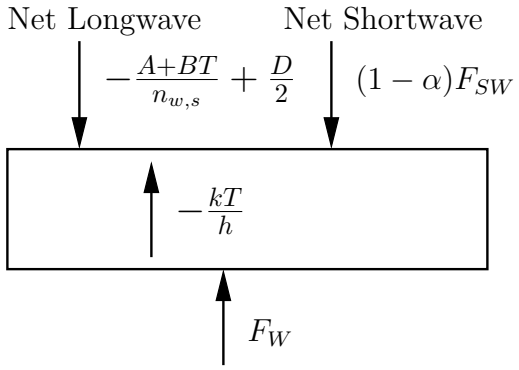

Figure 3. Flux balance of either winter or summer for the analytic method following the work of Thorndike [1992]. In summer T=0 and in winter F_{SW}=0. The subscript on the n is w for winter and s for summer. Definitions of variables are given in table 1.

Thorndike derived simple expressions for G and M by assumming they are proportional to the sum of the net flux incident on the top surface and the ocean heat flux incident at the base of the ice. He approximated the net surface flux from the seasonal mean, and he fixed the length of the growth and melt seasons each at one-half year. A schematic of the system is given in Fig. 3, from which Thorndike's equations follow:

$$G(h) = \frac{\tau}{L}\left[\frac{A+BT(h)}{n_w} - \frac{D}{2} - F_W\right] \qquad (1)$$

and

$$M = \frac{\tau}{L}\left[-\frac{A}{n_s} + \frac{D}{2} + F_W + (1-a)F_{SW}\right], \qquad (2)$$

both defined as positive quantities and T=0°C is assumed in Eq. 2. A list of variable definitions and default values is given in Table 1. Note that with these assumptions, only G is a function of h through its dependence on the surface temperature in winter:

$$T(h) = \left[\frac{n_w h}{k n_w + B h}\right]\left[-\frac{A}{n_w} + \frac{D}{2}\right]. \qquad (3)$$

Figure 4 shows curves for G and M taken from Eqs. 1–3 for two hypothetical "latitudes", which are distinguished soley by varying the mean flux of surface insolation F_{SW} (175 Wm^{-2} for 80°N and 200 Wm^{-2} for 68°N). We show curves for both a control climate, using the default values given in Table 1, and a perturbed climate, where A is decreased such that ΔA=-11.3 Wm^{-2}. The latter is meant to crudely approximate doubling CO_2 by increasing the downwelling longwave radiation on the annual mean at the surface by

$$\Delta F = -\frac{\Delta A}{2}\left(\frac{1}{n_w} + \frac{1}{n_s}\right) = 4 \text{ Wm}^{-2}. \qquad (4)$$

Figure 4 illustrates how the intersection of G and M defines $h_{\rm eq}$ for the control climate. Figure 4 also shows the change in G and M due to the increase in radiative forcing in the perturbed case, and the subsequent reduction in equilibrium thickness by $\Delta h_{\rm eq}$ that is required to establish a new balance between growth and melt.

Comparing the curves for the two hypothetical latitudes, $\Delta h_{\rm eq}$ is seen to be larger for the latitude with larger equilibrium thickness. This result is due to the thickness-dependence of the slope of G at $h_{\rm eq}$. Where the slope is steep, the ice need not thin very much to increase the annual growth and reastablish an equilibrium. In contrast, where the slope is shallow, the ice must thin comparably more to increase the annual growth. In other words, $\Delta h_{\rm eq}$ depends on the reciprocal of $\partial G/\partial h$, evaluated at $h_{\rm eq}$. Thorndike [1992] recognized that the response time for sea ice to adjust to equilibrium after a sudden change in thickness is equal to the reciprocal of $\partial G/\partial h$, evaluated at $h_{\rm eq}$. Hence $\Delta h_{\rm eq}$ and the response time depend on $h_{\rm eq}$ in a similar way.

The curves in Fig. 4 approximately agree with estimates for G and M for ice with $h_{\rm eq} = 3$ m given by Untersteiner [1961] and Maykut [1986] based on field data and modeling[1]. However, following Thorndike [1992], we have assumed M is independent of h, while Untersteiner [1961] and Maykut [1986] argue that M should increase if the ice becomes thin, say below 1 m, to account for the thickness-dependence of the ice albedo.

[1]We plot G and M as functions of the annual mean thickness, while Untersteiner [1961] and Maykut [1986] plot them against the thickness at the beginning of the season.

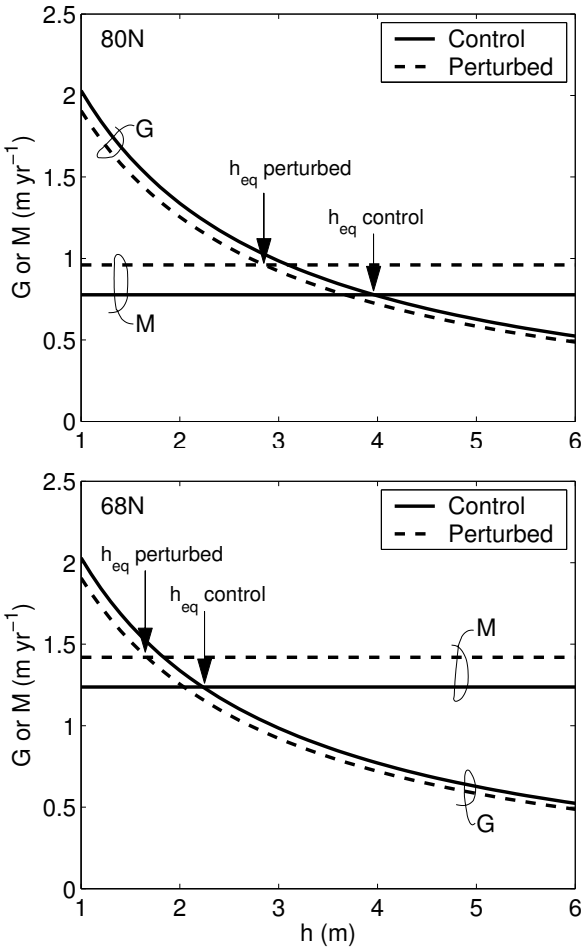

Figure 4. G and M versus h at 80 and 68°N for the control and perturbed cases of the analytic model.

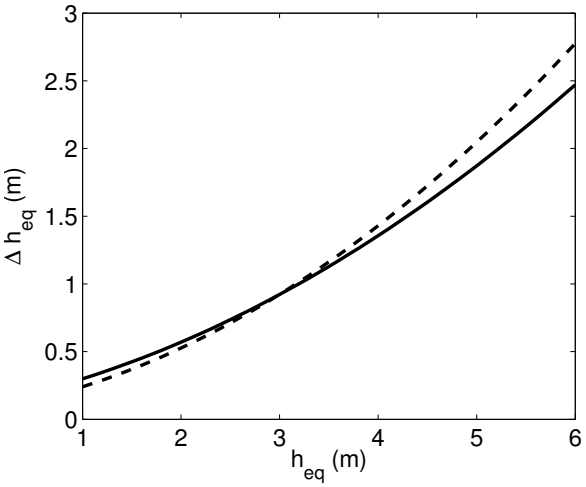

Figure 5. $\Delta h_{\rm eq}$ versus $h_{\rm eq}$ from the analytic model. The solid line uses the full expression in Eq. 7 and the dashed line is an approximation where $h_{\rm eq} = 3$ m for the term in brackets.

Fixing the length of the growth and melt seasons is another assumption that deserves further scrutiny. In real-

ity the season length depends on both ice thickness and the climate conditions. Owing to the simplifying assumptions made for this analysis, the quantitative predictions should not be taken too seriously, especially below 1 m.

The simplicity of Eqs. 1–3 allows an analytical solutions for $\Delta h_{\rm eq}$ as a function of $h_{\rm eq}$. This calculations yields a theoretical curve for comparing with the reduction in ice draft from the submarine data shown in Fig. 1 and the thickness change in the CMIP models (none of which are strictly in equilibrium, but can be considered to be in quasi-equilibrium because the response time for sea ice thickness change is short compared to the timescale of change to the forcing). When subject to a change in radiative forcing, sea ice reaches a new equilibrium by adjusting h such that $\Delta G = \Delta M$. An expansion in the dependent variables h and A that is linear in the change in thickness and the radiative perturbation gives

$$-\left.\frac{\partial G}{\partial h}\right|_{h_{\rm eq}} \Delta h_{\rm eq} + \left.\frac{\partial G}{\partial A}\right|_{h_{\rm eq}} \Delta A = \left.\frac{\partial M}{\partial A}\right|_{h_{\rm eq}} \Delta A, \qquad (5)$$

where $\Delta h_{\rm eq}$ is taken as positive for a reduction in ice thickness. Thus

$$\Delta h_{\rm eq} = -\left(\frac{\partial G}{\partial h}\right)^{-1}_{h_{\rm eq}} \left[\frac{\partial G}{\partial A} - \frac{\partial M}{\partial A}\right]_{h_{\rm eq}} \Delta A. \qquad (6)$$

Substitution from Eqs. 1–3 gives

$$\Delta h_{\rm eq} = -\frac{(k n_w + B h_{\rm eq})^2}{B n_w k(-A/n_w + D/2)} \left[-\frac{1}{n_w} - \frac{1}{n_s} + \frac{h_{\rm eq} B/n_w}{k n_w + B h_{\rm eq}}\right] \Delta A. \qquad (7)$$

In spite of the number of terms in this equation, the solution, shown as a solid line in Fig. 5, has a simple form. The term in brackets (in either Eq. 6 or 7) is only a weak function of thickness; therefore, our simple analytic model indicates $\Delta h_{\rm eq}$ approximately increases with the reciprocal of $-\partial G/\partial h$ (i.e., the response time). Indeed the dashed curve in Fig. 5 shows the thickness-dependence of $\Delta h_{\rm eq}$ from $(\partial G/\partial h)^{-1}$ alone by letting $h_{\rm eq} = 3$ m for the term within the brackets. With this approximation, $\Delta h_{\rm eq}$ is quadratic in $h_{\rm eq}$.

In Fig. 4 we distinguished latitudes by only varying F_{SW}, and hence neglected the spatial dependence of D. Continuing with this approximation, we can apply Eq. 7 to relate the spatial distribution of thinning to the initial thickness, as we did for the observed submarine data and CMIP model output. The magnitude of our estimate in Fig. 5 is not meant to be directly comparable to the CMIP models in Fig. 2 because the prescribed longwave forcing perturbation does not include feedbacks from other parts of the system, such as from clouds or water vapor.

It is convenient to combine Eq. 4 and 7 into the form

$$\Delta h_{\rm eq} = \lambda_h \Delta F \qquad (8)$$

where λ_h is a *thickness* sensitivity parameter. Eq. 8 is analogous to the relation $\Delta T_{\rm eq} = \lambda \Delta F$, where λ is known as the *climate* sensitivity parameter (see, e.g., IPCC 2001, p216) and is a measure of the ratio of the temperature change to the perturbative radiative forcing. By analogy, λ_h is a measure of the of the ratio of the thickness change to the perturbative forcing.

Feedback processes alter the magnitude of λ and λ_h. Others have recognized that the stabilizing effect of growth on ice thickness is a feedback process [e.g., Gordon and O'Farrell, 1997; Zhang et al., 2000; L'Heveder and Houssais, 2001]. Indeed, the growth-thickness relationship yields a feedback that is as basic to sea ice thickness as radiative emission is to temperature. However, the temperature-dependence of the climate sensitivity parameter due to radiative emission alone, $\lambda_0 = (4\epsilon\sigma T^3)^{-1}$ (ϵ is Earth's emissivity and σ is the Stefan-Boltzmann constant), is usually ignored, because the temperature dependence of λ_0 is not that great for the range of temperatures usually found on Earth. In contrast, according to Fig. 5, the thickness-dependence of λ_h from the growth-thickness relationship alone varies by at least a factor of two for thicknesses in the range of 1–6 m, which are typical of ice observed in the Arctic.

The thickness-dependence of this most basic feedback in sea ice gives rise to the dominant thickness-dependence of λ_h. Nonetheless, the thickness sensitivity parameter can easily be generalized to account for the thickness-dependence of M, as well as broader possibilities for the influence of radiative forcing on G and M (such as changes to the length of the melt or growth season):

$$\lambda_h = -\left[\frac{\partial G}{\partial h} - \frac{\partial M}{\partial h}\right]^{-1}_{h_{\rm eq}} \left[\frac{\partial G}{\partial F} - \frac{\partial M}{\partial F}\right]_{h_{\rm eq}}, \qquad (9)$$

which is still nonlinear in the thickness change and in the radiative perturbation. If we now account for ice-albedo feedback by letting M increase for small h, compared to the expression for $\Delta h_{\rm eq}$ in Eq. 7 (also see Fig. 5), $\Delta h_{\rm eq}$ would increase for small h. In the next section, we will present results from a numerical model that explicitly allows for ice-albedo feedback and other ice thermodynamics that were neglected here. In the section following that we discuss the implication of allowing ice dynamics as well.

4. Growth feedback in a simple numerical model

Here we recompute G and M using a numerical model that takes into account some of the important

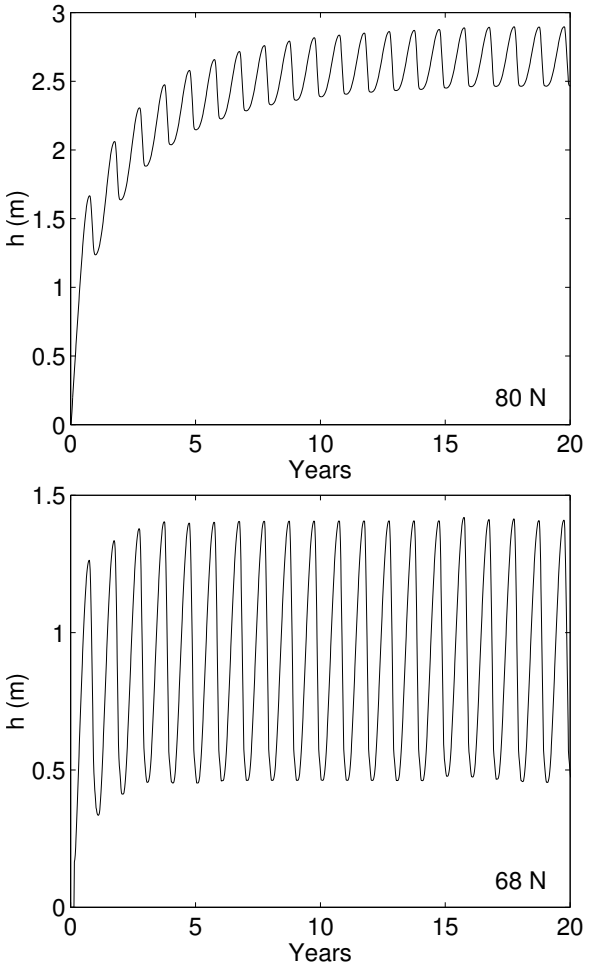

Figure 6. Timeseries of monthly mean ice thickness at 80 and 68°N from the EBM when initialized with zero-thickness ice.

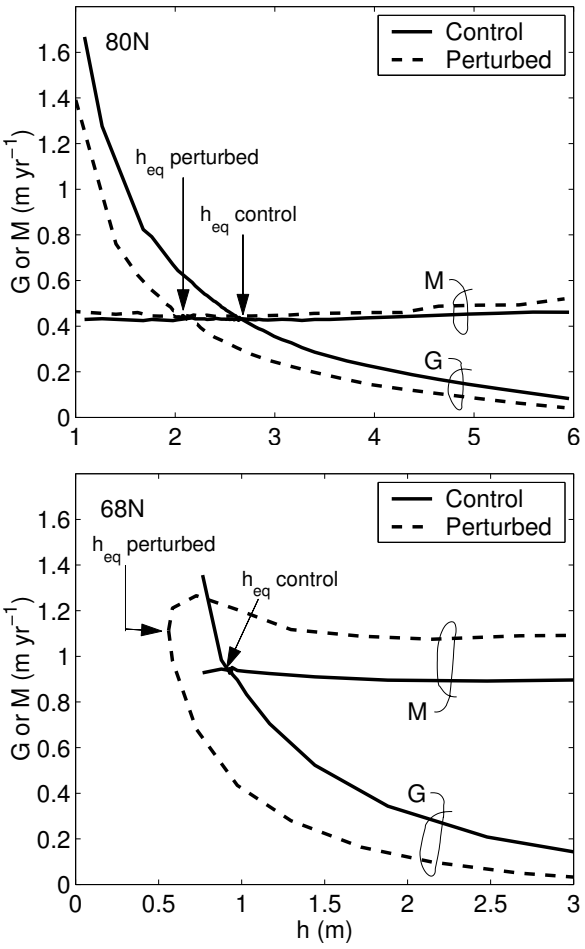

Figure 7. G and M versus annual mean h at 80 and 68°N from the EBM. These curves were constructed by taking the case shown in Fig. 6, where in the first year at 80°N, the mean ice thickess is 1.1 m, annual growth is 1.7 m and annual melt is .4 m. These values were then used here along with values taken from subsequent years and additions integrations. The approach to equilibrium at one latitude is coupled to other latitudes via the atmospheric and oceanic heat transport, and so long memory due to heat storage in the mixed layer corrupts the method a little, as seen by the slight noise in the curves.

processes that were neglected by the analytic model. In particular, we include a prognostic equation for the seasonal cycle of the energy balance of sea ice, a thickness-dependent albedo parameterization, a mixed-layer ocean, and variable heat transport in the atmosphere and ocean. For simplicity while exploring the thermodynamic mechanism outlined in the previous section, we use a model that lacks sea ice dynamics.

In keeping with the simple treatment of sea ice, we selected a model that lacks internal (and hence interannual) variability. The model is the seasonally-varying Energy Balance Model (EBM) of North and Coakley [1979], to which we added a prognostic equation for sea ice thickness, which is described in the Appendix. This zonal-mean model has fractions of land and ocean at each latitude, and it is forced with a seasonal distribution of solar heat entering the top of the atmosphere. Our parameterization for the planetary albedo over sea ice depends on h for $h < 1$ m.

For our control case, we use model equations and parameters from North and Coakley [1979], except as noted in the Appendix. We also ran the model with longwave radiation increased by 4 Wm^{-2} to mimic doubling CO_2, which we refer to as the perturbed case. We use 200 gridpoints evenly spaced in sine of latitude with mixed implicit and explicit numerical schemes to allow a timestep of 5 days.

Figure 6 illustrates the strong thickness-dependence of the response time in the EBM when initialized with zero-thickness sea ice. In agreement with Thorndike [1992], thicker ice takes longer to reach its equilibrium thickness. These figures also illustrate that the amount the ice grows in a single year is a strong function of

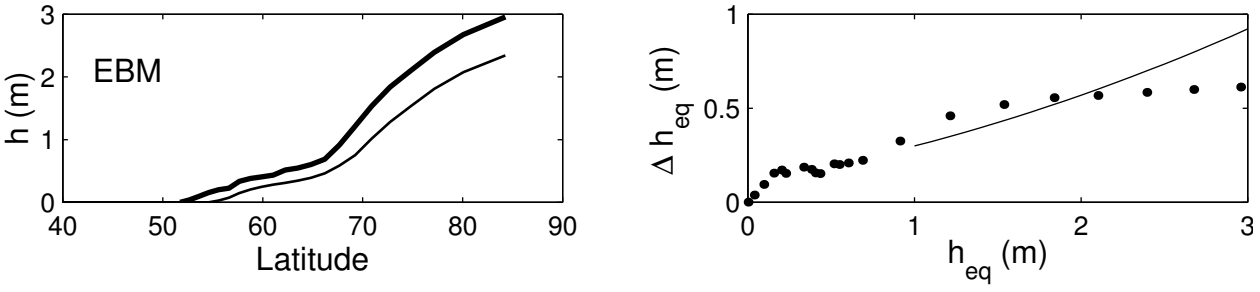

Figure 8. Thickness (left column) in the control (thick line) and perturbed (thin line) simulations from the EBM and corresponding scatter plot (right column) of the reduction in thickness as a function of the initial thickness for each gridcell in the northern hemisphere. The theoretical curve from Eq. 7 is reproduced on top of the EBM output on the right.

thickness. In contrast, the amount the ice melts in a single year is not very sensitive to thickness, although it does depend on latitude via the shortwave radiation.

Figure 7 shows estimates of G and M for 80 and 68°N derived from the EBM (see figure caption for an explanation). These curves resemble their counterparts from the analytic method, although the ice is somewhat thinner in the EBM. Under the perturbed conditions the ice at 68°N becomes seasonal, and so the intersection of G and M curves occurs at their endpoints. Even with a thickness dependent albedo parameterization, there is only a small increase in M for ice thinner than 1 m at 68°N. There is a small cusp near the endpoint of M at 68°N under the perturbed forcing as the ice becomes seasonal and there is less ice available to melt. Otherwise, for a given latitude and longwave forcing, M depends only weakly on thickness.

In the EBM, the change in M at a given latitude due to increased radiative forcing (i.e., $\partial M/\partial F$ in Eq. 9) is quite different for the two latitudes, and yet this possibility was neglected by the analytic model. We find $\partial M/\partial F$ is much larger at 68°N than 80°N in the EBM, as the albedo decreases and the ice becomes seasonal. In addition, storage of heat in the mixed layer and warming of nearby land at 68°N prolong the melt season by several weeks. In contrast, $\partial M/\partial F$ is very small at 80°N due to the reduction in the atmospheric and oceanic heat flux into the polar cap in a warmer climate. Thus $\partial M/\partial F$ in Eq. 9 is a function of latitude (and hence $h_{\rm eq}$) in the EBM. This dependence somewhat reduces the sensitivity of $\Delta h_{\rm eq}$ to $h_{\rm eq}$ compared to our estimates from the analytic model.

Figure 8 shows the thickness in the control and perturbed simulation as a function of latitude. In agreement with the CMIP models (see Fig. 2), the largest thickness reduction occurs within the central Arctic. Figure 8 also shows the thickness reduction as a function of the initial thickness from the EBM along with the theoretical estimate from Eq. 7. $\Delta h_{\rm eq}$ increases with $h_{\rm eq}$, but to a lesser extent than the theoretical curve, as expected due to ice-albedo feedback and other neglected physics in the analytic model.

The results from the EBM suggests that neglected processes in the analytic model can have a sizeable influence. Although the growth-thickness feedback still dominates the results. In the discussion which follows we consider the influence of ice dynamics.

5. Discussion of the role of ice dynamics

We have used very simple models to investigate a mechanism inherent in sea ice thermodynamics that can cause sea ice to thin most where it was initially the thickest, when subject to increased radiative forcing. In reality sea ice does not last long enough in a single location to attain an equilibrium. Additionally, in an Eulerian perspective, we must account for net outflow O from a given region (i.e., the volume divergence averaged over the region) in our volume budget [see Hibler and Hutchings, 2002]. Hence $G - M - O = 0$, defines a quasi-equilibrium state for sea ice in motion. Our equation for the thickness sensitivity parameter then becomes

$$-\lambda_h = \left[\frac{\partial G}{\partial h} - \frac{\partial M}{\partial h} - \frac{\partial O}{\partial h}\right]^{-1}_{h_{\rm eq}} \left[\frac{\partial G}{\partial F} - \frac{\partial M}{\partial F} - \frac{\partial O}{\partial F}\right]_{h_{\rm eq}}. \quad (10)$$

The component of λ_h within the first brackets (including the exponent) is the response time, which depends on the thickness-dependence of the volume budget terms. The component within the second brackets represents the response of the volume budget terms to the climate forcing.

In an investigation of the potential for multiple equilibria in sea ice, Hibler and Hutchings [2002] estimated the thickness-dependence of O averaged over

the whole Arctic Basin using an idealized dynamic-thermodynamic sea ice model. They found O is roughly linear in h for $h < 2$ m, when the ice can be considered rather weak[2], and O reaches a maximum at about 3 m and decreases for larger h, as the ice strength begins to noticeably build with h. If we assume this estimate for O also applies on say the spatial area of the submarine crossing or the grid area in the CMIP models, then the contribution from $\partial O/\partial h$, roughly speaking, would reduce $\Delta h_{\rm eq}$ for $h < 2$ m but increase it for $h > 4$ m. Therefore, the thickness-dependence of O would make $\Delta h_{\rm eq}$ increase even more steeply with $h_{\rm eq}$, compared to our estimates from either the analytic model or the EBM.

Recent trends in the ice circulation [see e.g., Steele et al., 1996; Tucker et al., 2001; Rigor et al., 2002] due to trends in the atmosphere (or ocean) circulation can be considered part of the response to climate forcing, and hence can be accounted for in our equations with $\partial O/\partial F$. One can imagine a trend in the winds or ocean stresses could be correlated in space with the pattern of sea ice thickness, which could, either by coincidence or due to some kind of coupled response, yield a thickness-dependence in $\partial O/\partial F$. While we know of no study that has shown estimates of $\partial O/\partial F$ as a function of h, sea ice hindcast with models forced by observed atmospheric conditions indicate that the recent thickness change can be mainly attributed to trends in the winds [Zhang et al., 2000; Holloway and Sou, 2002; Köberle and Gerdes, 2003]. According to Eq. 10, $\partial O/\partial F$ multiplies the portion of $\Delta h_{\rm eq}$ that is due to the thickness-dependence of G and the other terms in volume budget, and the thickness-dependence of this latter portion was the main focus of this study.

6. Conclusions

We have shown that the spatial distribution of sea ice thinning over the past few decades in the central Arctic as measured by submarines was a strong function of the initial draft. A similar relationship is reproduced individually by CMIP models when sea ice thins in response to increased levels of CO_2 in the models' atmosphere. Moreover, because many of the CMIP models have only weak trends in their surface winds and several models lack ice dynamics altogether, the explanation of the models' behavior likely rests on ice thermodynamics.

We described a mechanism to explain the thickness-dependence of the thickness change in response to a radiative perturbation by building upon an existing theory of sea ice mass balance from Thorndike [1992]. One of the predictions from Thorndike [1992] is that the rate at which sea ice can respond to a perturbation of its thickness will depend upon the growth adjustment process. The growth-thickness relationship defines a feedback process that rapidly returns thin ice to its equilibrium thickness when it is subject to a single abrupt thickness perturbation, but leads to thicker ice spending more time away from its equilibrium. When subject to an increase in radiative forcing, the annual melt will increase and annual growth will decrease. In response, the ice must thin until the annual growth balances the annual melt again. Because the growth rate of thin ice increases very rapidly when the ice thins further, thin ice need not thin much to attain a new equilibrium thickness, while thicker ice must thin more. Using simple expressions for annual growth and melt from Thorndike [1992], we estimated a theoretical relationship for the thickness change, which we found to increase approximately quadratically with thickness.

One might imagine that a strong positive feedback, such as ice-albedo feedback, would dominate the thickness-dependence of the response to radiative perturbations. But ice-albedo feedback ought to cause thin ice to melt more, which is the opposite thickness-dependence to what is observed by submarines and simulated in CMIP models. Compared to our estimates for the growth-thickness feedback alone, adding ice-albedo feedback tends to slightly level out the the slope of the curve relating the thickness change to the initial thickness.

We compared our theoretical estimates to results from a simple zonal-mean, energy balance model that explicitly included sea ice with ice-albedo feedback but lacked ice dynamics. The growth-thickness feedback controls the overall behavior, although ice-albedo feedback and variable season lengths have a nontrivial influence on the model results.

We generalized our theoretical framework to account for both sea ice dynamics and climate perturbations that include trends in the wind or ocean stress. Based on estimates from Hibler and Hutchings [2002], we argued that ice dynamics would likely reduce the thickness change for ice that is in free drift, or nearly so, and increase the thickness change for ice that has considerable compressive strength. This transition can be associated with an ice thickness of about 3m. Thus generally ice dynamics would steepen the slope of the curve relating the thickness change to the initial thickness, compared to the relationship predicted with simple growth-thickness feedback alone.

In agreement with several other studies, comparing the rate of thinning observed by the submarines with the thinning in response to doubling CO_2 in CMIP models suggests that recent trends in the atmospheric circulations were critical in explaining the submarines measurements. In spite of the likely differences in the

[2]The net outflow for a region is the divergence of the volume flux: $O = \nabla \cdot h\mathbf{v}$ averaged over the region, where $\mathbf{v}$ is the ice velocity. If the wind and ocean stresses are independent of sea ice thickness and we consider the ice to be in free drift, we can assume $\mathbf{v}$ is nearly independent of h, then O is roughly proportional to h.

source of the thickness perturbation (i.e., suface radiative fluxes in the CMIP models and mostly wind stress in the submarine measurements), the thinning increases sharply with thickness in both the CMIP models and in submarine measurements. The results from the CMIP model suggest that sea ice thinning in the future will be a strong function of thickness in response to increased levels of carbon dioxide in the atmosphere, even if trends in the atmospheric circulation do not continue.

Our results indicate that when a climate perturbation causes the ice to thin, the greatest thinning occurs in the central Arctic, where the ice is thickest, and less thinning occurs in the subpolar seas. An estimate of the overall thickness change in the Arctic should take into account the strong thickness-dependence of the change. For this reason, it is important to accurately measure and simulate the ice thickness to better understand the past and future of the Arctic ice pack.

Acknowledgments. We thank Drs. Rothrock and Flato and one anonymous reviewer for their constructive reviews. We thank Drs. Gregory and Moritz for helpful comments and suggestions. Dr. Y Yu provided the submarine data used in Fig. 1. Dr. G. Schmidt provided direct radiative forcing estimates for the 20th century from Hansen et al. (2002). Participating CMIP modeling groups for providing data on sea ice thickness and extent to the CMIP model archive. CMB gratefully acknowledges the support of the National Science Foundation, Office of Polar Programs grant number OPP0084287.

Appendix

The energy balance model, developed by North and Coakley [1979], simulates the seasonal cycle of land and ocean temperature. In the presence of sea ice, the energy balance is identical to the balance over ocean surfaces except the time rate of change of heat storage in the ocean is replaced by the conductive flux through the top surface of the sea ice:

$$-k\frac{T_b - T_s}{h} = Q(x,t)(1-\alpha_s) - (A + BT_s) + \eta\frac{d}{dx}D(1-x^2)\frac{dT_s}{dx} - \frac{\nu}{f_W}(T_s - T_L), \quad (11)$$

where x is the sine of latitude, k is the conductivity, Q is the solar heating, T_s is the surface temperature, T_b =-2°C is the freezing point of sea water, α_s is the planetary albedo over sea ice, $A+BT_s$ is the net outgoing infrared radiations, D is the diffusivity (taken to be a function of x following Lindzen and Farrell [1977]), f_W is the fraction of the latitude covered by ocean, ν controls land–ocean heat exchange, and T_L is the temperature of the fraction of the latitude covered by land. Note that parameters A, B, and D used for the EBM are similar but not equivalent to the one used for the analytic calculations in Section 3. The surface temperature T_s is constrained to be at or below T_b. The last term of the right-hand-side of Eq. 11 represents the land-ocean coupling in the EBM, which is necesary in a seasonal model [North and Coakley, 1979]. The coefficient η is used to separate the meridional heat flux into atmospheric and oceanic portions in the presence of sea ice only, where we let the top surface of the ice receive 95% and the other 5% is applied to the base of the ice, as the variable F_W in Eq. 12. These percentiles are based on estimates at 60°N and 60°S from the work of Trenberth and Caron [2001].

The instantaneous growth (or melt) rate of sea ice is computed from

$$\rho L_f \frac{\partial h}{\partial t} = F_{\rm net} - F_W \quad (12)$$

where $F_{\rm net}$ is equal to the right hand side of Eq. 11. We make a special calculation anytime the ocean temperature drops below T_b point, where we grow just enough ice to bring the temperature back to T_b, and adjust h accordingly. By assuming the vertical temperature in the ice is always linear, the heat capacity of sea ice is neglected in this model.

The planetary albedo over snow-free land and ice-free ocean is

$$\alpha_{L,W} = 0.3 + 0.04(3x^2 - 1). \quad (13)$$

Land is considered snow covered ($\alpha_L = 0.6$) when $T_L \leq$-2°C or south of 65°S. The planetary albedo over sea ice is

$$\alpha_s = \alpha_W(1-\gamma) + 0.6\gamma, \quad (14)$$

where $\gamma = ln(100h)/ln(100)$ for $h < 1$ m and otherwise $\gamma = 1$. The logarithmic dependence is based on the work of Ebert and Curry [1993].

References

Briegleb, B. P., C. M. Bitz, E. C. Hunke, W. H. Lipscomb and J. L. Schramm, 2002: *Description of the Community Climate System Model Version 2 Sea Ice Model.* http://www.ccsm.ucar.edu/models/ccsm2.0/csim/, pp. 60.

Cubasch, U., R. Voss, G. C. Hegerl, J. Waszkewitz and T. J. Crowley, 1997: Simulation of the influence of solar radiation variations on the global climate with an ocean-atmosphere general circulation model. *Clim. Dyn.*, **13**, 757–767.

Ebert, E. E. and J. A. Curry, 1993: An intermediate one-dimensional thermodynamic sea ice model for investigating ice-atmosphere interactions. *J. Geophys. Res.*, **98**, 10085–10109.

Flato, G. M., 2004: Sea-ice climate and sensitivity as simulated by several global climate models. submitted to Clim. Dyn.

Gillett, N. P., M. Allen, R. E. McDonald, C. A. Senior, D. T. Shindell and G. A. Schmidt, 2002: How linear is the Arctic Oscillation response to greenhouse gases? *J. Geophys. Res.*, **107**, ACL 1–1–1–7, 0.1029/2001JD000589.

Gordon, C., C. Cooper, C. A. Senior, H. T. Banks, J. M. Gregory, T. C. Johns, J. F. B. Mitchell and R. A. Wood, 2000: The simulation of SST, sea ice extents and ocean heat transports in a version for the Hadley Centre coupled model without flux adjustments. *Clim. Dyn.*, **16**, 147–168.

Gordon, H. B. and S. P. O'Farrell, 1997: Transient climate change in the CSIRO coupled model with dynamics sea ice. *Mon. Wea. Rev.*, **125**, 875–907.

Hansen, J. and 27 others, 2002: Climate forcings in Goddard Institute for Space Studies SI2000 simulations. *J. Geophys. Res.*, **107**, doi:10.1029/2001JD001143.

Hansen, J., G. Russell, A. Lacis, I. Fung and D. Rind, 1985: Climate response times: Dependence on climate sensitivity and ocean mixing. *Science*, **229**, 857–859.

Hibler, W. D. and J. K. Hutchings, 2002: Multiple equilibrium arctic ice cover states induced by ice mechanics. in *Ice in the Environment: Proceedings of the 16th IAHR International Symposium on Ice*, Vol. Dunedin, New Zealand, Dec. 2002., pp. 228–237.

Holland, M. M. and C. M. Bitz, 2003: Polar amplification of climate change in the Coupled Model Intercomparison Project. *Clim. Dyn.*, **21**, 221–232.

Holloway, G. and T. Sou, 2002: Has arctic sea ice rapidly thinned? *J. Climate*, **15**, 1691–1701.

IPCC, 2001: *IPCC third assessment report: Climate change 2001: The scientific basis*. Cambridge University Press, Cambridge, UK, 944pp.

Köberle, C. and R. Gerdes, 2003: Mechanisms determining the variability of arctic sea ice conditions and export. *J. Climate*, **17**, 2843–2858.

Kolesnikov, A. G., 1958: On the growth rate of sea ice. in *Proc. from Arctic Sea ice, Easton, Maryland, Feb. 24–27, 1958*, pp. 157–161.

L'Heveder, B. and M.-N. Houssais, 2001: Investigating the variability of the arctic sea ice thickness in response to a stochastic thermodynamic atmospheric forcing. *Clim. Dyn.*, **17**, 107–125.

Lindzen, R. S. and B. Farrell, 1977: Some realistic modifications of simple climate models. *J. Atmos. Sci.*, **34**, 1487–1501.

Maykut, G. A., 1986: The surface heat and mass balance. in N. Untersteiner, editor, *The Geophysics of Sea Ice*, Vol. 146, pp. 395–463. NATO ASI Series B, Physics, Plenum, New York, London.

Meehl, G. A., G. Boer, C. Covey, M. Latif and R. Stouffer, 2000: Coupled Model Intercomparison Project. *Bull. Amer. Meteor. Soc.*, **81**, 313–318.

North, G. R. and J. A. Coakley, Jr, 1979: Differences between seasonal and mean annual energy balance model calculations of climate and climate sensitivity. *J. Atmos. Sci.*, **36**, 1189–1204.

Rigor, I. G., J. M. Wallace and R. L. Colony, 2002: Response of sea ice to the Arctic Oscillation. *J. Climate*, pp. 2648–2668.

Rothrock, D. A., Y. Yu and G. A. Maykut, 1999: Thinning of the arctic sea ice cover. *Geophys. Res. Lett.*, **23**, 3469–3472.

Rothrock, D. A., J. Zhang and Y. Yu, 2003: The arctic ice thickness anomaly of the 1990s: A consistent view from observations and models. *J. Geophys. Res.*, **108**, doi:10.1029/2001JC001208.

Semtner, A. J., 1976: A model for the thermodynamic growth of sea ice in numerical investigaions of climate. *J. Phys. Oceanogr.*, **6**, 379–389.

Steele, M., D. Thomas, D. Rothrock and S. Martin, 1996: A simple model study of the arctic ocean freshwater balance. *J. Geophys. Res.*, **101**, 20,833–20,848.

Thorndike, A. S., 1992: A toy model linking atmospheric thermal radiation and sea ice growth. *J. Geophys. Res.*, **97**, 9401–9410.

Trenberth, K. E. and J. M. Caron, 2001: Estimates of meridional atmosphere and ocean heat transports. *J. Climate*, **14**, 3433–3443.

Tucker III, W. B., J. W. Weatherly, D. T. Epller, D. Farmer and D. L. Bentley, 2001: Evidence for rapid thinning of sea ice in the western Arctic Ocean at the end of the 1980s. *Geophys. Res. Lett.*, **28**, 2851–4.

Untersteiner, N., 1961: On the mass and heat budget of arctic sea ice. *Arch. Meteorol. Geophys. Bioklimatol., A*, **12**, 151–182.

Untersteiner, N., 1964: Calculations of temperature regime and heat budget of sea ice in the Central Arctic. *J. Geophys. Res.*, **69**, 4755–4766.

Wadhams, P. and N. R. Davis, 2000: Further evidence of ice thinning in the arctic ocean. *Geophys. Res. Lett.*, **27**, 3973–5.

Zhang, J., D. Rothrock and M. Steele, 2000: Recent changes in Arctic sea ice: The interplay between ice dynamics and thermodynamics. *J. Climate*, **13**, 3099–3114.

C. M. Bitz, Polar Science Center, MS 355640, University of Washington, Seattle, WA 98105-5640. (bitz@apl.washington.edu)

G. H. Roe, Earth and Space Sciences, MS XXXXX, University of Washington, Seattle, WA 98195-1360. (gerard@ess.washington.edu)

Received July 3, 2003; revised Jan 14, 2004; accepted X Y, 2004.